Article

Pannonian Basin Nocturnal Boundary Layer and Fog Formation: Role of Topography

Joan Cuxart [1,*], Maja Telisman Prtenjak [2] and Blazenka Matjacic [3]

1. Department of Physics, University of the Balearic Islands, 07122 Palma de Mallorca, Spain
2. Department of Geophysics, Faculty of Science, University of Zagreb, 10000 Zagreb, Croatia; telisman@gfz.hr
3. Meteorological and Hydrological Service (DHMZ), 10000 Zagreb, Croatia; blazenka.matjacic@dhz.hr
* Correspondence: joan.cuxart@uib.cat

Abstract: Under high-pressure systems, the nocturnal atmospheric boundary layer in the Pannonian Basin is influenced by gravity flows generated at the mountain ranges and along the valleys, determining the variability of wind and temperature at a local scale and the presence of fog. The mechanisms at the mountain foothills are explored at Zagreb Airport using data from a sodar and high-resolution WRF-ARW numerical simulations, allowing identification of how the downslope flows from the nearby Medvednica mountain range condition the temperature inversion and the visibility at night and early morning. These flows may progress tens of kilometres away from the mountain ranges, merging with valley flows and converging in the central areas of the basin. The ECMWF model outputs allow us to explore the mesoscale structures generated in form of low-level jets, how they interact when they meet, and what is the effect of the synoptic pressure field over eastern Europe, to illustrate the formation of a basin-wide cold air pool and the generation of fog in winter.

Keywords: Pannonian Basin; nocturnal atmospheric boundary layer; low-level jets; downslope flows; fog; basin-scale flows

1. Introduction

Large areas with low elevation relative to their surroundings in emerged land are rarely flat, even if they seem otherwise to the human eye. Very gentle slopes are normally present, and microscale topographical variability generates shallow depressed zones with local minimal temperatures. Furthermore these almost-flat lands are usually confined by some significant topography over which slope flows develop in appropriate meteorological conditions, usually reaching the low lands and determining the dynamics of the atmospheric boundary layer (ABL) and the local climatology.

The characteristics of the interaction of flows originating at mountain ranges and over adjacent plains in the Pannonian Basin at night and their role in the generation of fog are the subjects of this study. This eastern European region has become the subject of detailed investigations under the umbrella of the PannEx initiative [1], that aims to study the basin in an integrated matter for agro-climatological [2–5] and hydrometeorological [6,7] purposes in the frame of the ongoing climate change. In particular, we aim to analyse, in detail, the phenomena in the area of the foothills of the Medvednica mountain range, where fog is a recurrent feature needing better understanding [8], and to see how flows organise in the plain, well away from the mountain ranges [9].

In situations when the synoptic pressure gradients over the basin are weak, nocturnal local flows develop over topography [10]. Over mountain ranges, well-defined downslope flows develop that can blow over the foothills and, if not impeded, progress further away becoming mesoscale structures as it has been found for several basins [11,12]. These conditions allow the development of significant spatial heterogeneities at small scales, locally modifying the values of the meteorological variables near the surface but without altering

significantly the structure of the mesoscale flows [13], unless the spatial heterogeneity itself is of mesoscale dimension [14].

Stably stratified nights under anticyclonic conditions are a very common event, and there seems to be a trend to increase their frequency in the last decades for the Pannonian Basin [15,16]. These situations, ruled at each location by local or mesoscale winds, are prone to strong surface radiative cooling and the development of a surface-based thermal inversion in which near-the-surface temperatures may fall significantly along the night. In these conditions, pollutants remain trapped in the thermal inversion posing a threat to public health [17,18] and ecosystems [19].

In surface thermal inversions, saturation may occur near the surface in calm conditions leading to dew formation or fog. Fog is called of radiative origin when the surface cooling combined with weak turbulence generates a relatively shallow fog layer that may increase depth along the night [20]. Instead, stronger turbulent mixing may generate deep fog layers in a more sudden manner, for instance when a well-mixed turbulent layer becomes saturated as temperature decreases and fog is formed in all its depth [21].

In winter, deep fog layers are difficult to dissipate in the daytime, resulting in persistent fog events lasting several days until general meteorological conditions change [22]. In these situations, the fog layer is capped by a thermal inversion at a height of a few hundred metres, a layer where atmospheric pollutants will cumulate along the episode [23], with concentrations that may reach values close or above the authorised limits [24].

The present investigation deals with the generation of mesoscale gravity flows by the topography in the Pannonian Basin and their influence on the stably stratified ABL (SBL), with special interest on fog formation. The first part looks with detail at one point at the foothills of the mountain ranges, Zagreb Airport, where fog is often observed [25], following the line opened by Telisman Pretenjak et al. [8], that inspected how the presence of downslope flows could influence the formation of fog on the flat areas at the foothills of the Medvednica mountain range. The second part proceeds to inspect the same features at the basin scale, in which the focus is put on the organisation of the flows at mesoscale. The analysis is made combining numerical model outputs and available data in the area. The intention is to identify the relevant mechanisms in fog formation under high-pressure conditions, assessing which of them dominate and under which conditions. We expect shallow radiation fog to appear in weak wind conditions and fog created by turbulent mixing when low-level jets (LLJs) are in place.

The manuscript displays the tools and methods used in Section 2, while Section 3 focuses on the effect of the arrival of gravity flows on the foothills and their role in the generation of fog, making use of a high-resolution mesoscale simulation with the WRF-ARW model and data at the airport, including sodar vertical profiles. Section 4 takes the wider perspective of the whole basin, for which outputs from the ECMWF mode and operational observational data are analysed. Finally, Section 6 provides some conclusions and reflects on the perspectives to further study these meteorological features.

2. Data and Methodology

2.1. Geographical Description

The Pannonian Basin is commonly thought of as a large plain along which the Danube flows between Vienna and the Iron Gates, in which are found some of its more important tributaries (Tisza on the left and Sava, Drava, and Great Morava on the right). It is limited by the Eastern Alps to the W, the Dinarides to the S, and the Carpathians to the N and E, enclosing a large plain (Alföld) to the W and the Transylvanian elevated area to the NE, with average elevations of 100 and 400 m above sea level (asl), respectively (Figure 1a). The average distance from Szeged, at the centre of the plain, to the initial slopes of the topography enclosing the basin or Transylvania is about 150 km.
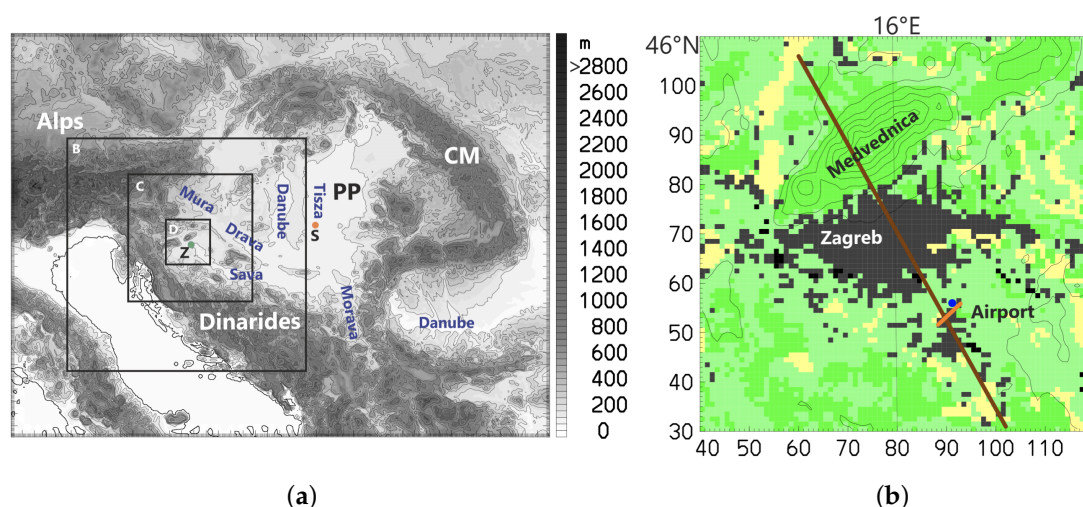
Figure 1. (**a**) The Pannonian Basin with indication of the 3 inner embedded domains of the WRF-ARW simulation, with the main topographical features (PP: Pannonian Plain, CM: Carpathian Mountains), some river names in blue, and Zagreb (Z) and Szeged (S). (**b**) The Zagreb Airport area, with the city to the NNW and the Medvednica mountain range to the NW–NNE. The orange bar indicates the runway of the airport and the blue circle the location of the sodar.

In the northeastern extreme of the Pannonian Basin, the capital city of Croatia, Zagreb, is on the southern slopes of Medvednica Mountain (Figure 1b), which extends approximately 40 km in the NE–SW direction with a width of 10 km, reaching the highest peak at 1035 m asl. About 20 km southward from Medvednica is Zagreb Airport (45.73° N, 16.06° E; 108 m asl), located in the lowland region near the Sava river, which is rich with underground waters and mostly covered by grass and small forests. The configuration of a steep slope in Medvednica mountain with flat foothills open to the centre of the basin makes of it an ideal location for the study of the initial stages of mountain–plain interaction, benefiting from the presence of a permanent meteorological station at the airport.

2.2. Observations

Routine meteorological observations are made in Zagreb Airport, especially aeronautical half-hourly METAR reports giving information on the weather conditions that include meteors, visibility, wind at 10 m above ground level (agl), and temperature and humidity at 2 m agl.

Between 2016 and 2018, a Scintec MFAS sodar of the Hydrometeorological Service of Croatia was installed in the northern side of the airport close to the runway, with a shield around it to protect the measurements from ambient acoustic contamination, mostly from a nearby highway. The sodar functioned with a number of interruptions lasting between days and weeks, allowing meteorological events to be studied but not the performance of meaningful statistics. The sodar was set to produce vertical profiles of virtual temperature, wind speed and direction, and estimations of turbulence from 30 to 300 m agl, at a resolution of 30 m, with averaging and output intervals of 10 min.

At the full Pannonian Basin scale, data from the operational network of the official Meteorological Services of the countries of the basin have been used, as far as they were available in ECMWF Meteorological Archival and Retrieval System (MARS). Data employed were specifically the meteorological reports at official stations and the profiles from radiosondes. In this manuscript, we have shown data from Zagreb Airport and also from the Szeged aerodrome, mainly to assess the ECMWF model behaviour in the central part of the basin.

2.3. Numerical Simulations

Model outputs from two numerical models were used. On the one hand, the ECMWF analyses and forecasts at a temporal resolution of 3 h were inspected, which have an

approximate horizontal resolution of 9 km. Analysis fields were used with preference, corresponding to 00, 06, 12, and 18 UTC, also inspecting forecast fields when convenient. While ECMWF most of the time is represented with good approximation, regarding the weather in the Pannonian Basin when a high-pressure system is over the area, local details are sometimes not well captured, especially concerning low clouds and fog related to small-scale terrain features.

To obtain a view of the processes at a smaller scale than the one provided by ECMWF, a simulation with the WRF-ARW (Weather and Research Forecasting—Advanced Research version) model was performed, using ECMWF fields as initial and lateral boundary conditions. This is a non-hydrostatic state-of-the-art mesoscale atmospheric numerical model [26] which solves the fully compressible, non-hydrostatic equations of motion in an Arakawa-C grid with the terrain following vertical coordinates. The model is run with the same configuration for the Zagreb region as in Telisman Prtenjak et al. [8], and the setup characteristics are given in Table 1, while the three innermost two-way nested domains are shown in Figure 1a. Here, we will concentrate on the outputs from the innermost domain at a resolution of 500 m, also taking advantage of a well-resolved ABL (25 levels in the first kilometre agl).

Depending on the resolution, the models may have a more precise representation of the topography. The Medvenica mountain range is well represented in WRF-ARW at high resolution, while the same area is seen as a part of a sustained slope starting further east in ECMWF. Therefore, WRF-ARW is the adequate tool to inspect local effects near the topography, while ECMWF can describe correctly the effects at mesoscale as the resolution adequately captures the altitudinal contrast between the slopes and the plain, even if the specific details may not be representatively locally.

Table 1. Parameters of the WRF simulation.

Radiation	Shortwave [27] Longwave RRTM [28]
Cumulus	Betts–Miller–Janjic [29] (largest domain only)
Microphysics	2 moment [30]
Land Surface	5 layer [31]
ABL	MYNN [32]
Urban scheme	Single-layer UCM [33]
Type of domains	4(A–D) two-way nested
Domain A	110 × 100 points (E–W, N–S) 13.5 km × 13.5 km
Domain B	118 × 118 points (E–W, N–S) 4.5 km × 4.5 km
Domain C	163 × 163 points (E–W, N–S) 1.5 km × 1.5 km
Domain D	154 × 154 points (E–W, N–S) 0.5 km × 0.5 km
Vertical grid: semi-sigma levels up to 1 km above ground	5, 16, 28, 41, 67, 81, 95, 110, 125, 142, 159, 177, 195, 215, 235, 256, 278, 302, 328, 369, 433, 525, 663, 838, 1025...

The model parameterisations for several categories of physical processes (i.e., longwave and shortwave radiation, soil model, cumulus clouds, microphysics, surface layer, ABL and turbulence) are also displayed in Table 1, as in other fog-oriented modelling studies with the same model [34–36]. Cumulus parameterisation was applied only in the largest domain. Topographic and land-cover data came from the 90 m resolution of the SRTM (Shuttle Radar Topographic Mission) digital topographic database and the 100 m res-

olution CORINE (Coordination of Information on the Environment Land Cover) database, respectively. Initial and lateral boundary conditions were taken from the ECMWF analyses at a resolution of 0.125° every 6 h. The simulations lasted 48 h and started at noon on the 27 January 2018, taking into account the spin-up time (here considered to be the first 6 h).

2.4. Strategy of Analysis

To analyse the effect of the downslope flows on the SBL at the foothills of the Medvednica mountain range and their contribution to fog formation and evolution in Section 3, the days when the sodar was operative have been inspected. Two episodes of interest were selected for which the METAR and sodar data were analysed, complementing the analysis with the outputs of the numerical simulations.

The first episode corresponds to the period between noon of 17 September 2017 and noon of the next day, when downslope flows reached the airport with intermittent fog events. In this case, we used the outputs of the ECMWF model since they were able to reproduce the formation and evolution of the fog events with good approximation.

The second episode comprises two consecutive winter nights, 27–28 and 28–29 January 2018. The first night presents the development of downslope flows once the general winds weaken from midnight and during three hours, arriving over the airport in the foothills, with formation of mist and light fog. The next night, a cloudy nocturnal ABL was covered by stratocumulus that extended very close to the ground generating fog, and the downslope flows interact with the clouds, especially at their top. These phenomena are of very small scale, and high-resolution WRF model outputs are used to analyse the mechanisms in place.

In Section 4, the interest is on the organisation of the ABL at the mesoscale and the basin scale. This is performed with selected ECMWF model outputs between August and December 2016, and comparison with the data for the Aerodrome of Szeged in Hungary. While the main features at the basin scale are illustrated using the analyses for four selected days at midnight, the vertical structure is inspected for one summer day and one winter day both with clear skies, and for an event of low Sc and fog covering most of the basin.

In Section 5, the interpretation of the events above is made, connecting the conceptual model developed from the events at the foothills with those inferred from the analysis at the basin scale, paving to the way to an ensemble view of all these structures. Finally, the main conclusions and some perspectives are given in the final section.

3. Slopes and Foothills

Motivated by understanding the origin of some fog events at Zagreb Airport on the Sava plain at about 20 km distance from the Medvednica mountain range, Telisman Prtenjak et al. [8] analysed two consecutive November nights by means of a high-resolution numerical simulation. The analysis of the model outputs indicated that there are different fog mechanisms in play depending on whether the downslope flows reach the foothills or not.

When gravity flows do not progress over the plain, most likely because they experience a hydraulic jump, the valley dynamics with SW flows dominate and an initially shallow radiation fog may develop in a well known situation associated with fog at the airport station [25] during the so-called 'fog season' (September–April). In the second night, the arrival of downslope flows at the airport was related to a sudden fog formation event, deeper than in the previous night, related to the mixing caused by the arrival of the gravity flow.

The presence of a sodar in Zagreb Airport has allowed continued exploration of the interaction between downslope flows and fog events in the foothills, making use of the information on the vertical structure of the first tens of meters above the surface. The available database has been explored and a small number of cases selected, taking into account that it is difficult to find quasi-ideal situations in reality. Three night events have been chosen for the analysis, one in late summer and two in winter. The two first cases

illustrate how katabatic flows may generate fog or dense mist events over the foothills, while the third has a compact Sc deck that interacts with the downslope flows.

3.1. Intermittent Generation of Fog in Summer by Gravity Flows

The 17–18 September 2017 case had the Zagreb area near the centre of a large high-pressure system with very weak general SW flows. According to the METAR reports (Figure 2a), the wind blows from SW from 12 to 02 UTC with decreasing speed (2 m/s in the afternoon, 1 m/s to calm in the evening and early night), with a sustained decrease in temperature under clear skies. Between 02 and 12 UTC, the wind oscillates between calm and northerly flow, humidity becomes saturating near the surface, and there is intermittent formation of fog.

The dynamical picture of this event becomes clearer when additionally inspecting the wind profiles from the sodar (Figure 2b,c). Before 02 UTC, the wind essentially blows from SW at all levels with decreasing speed, and the wind speed at 90 m agl is larger than at 30 m agl. Afterwards, the wind direction is from the first quadrant (N to E) and the wind speed is often larger at 30 than at 90 m agl, which indicates the presence of a LLJ coming from the direction of Medvednica. The presence of transient fog episodes takes place as this regime is established late night and early morning, very likely due to turbulent mixing fog induced by the gravity flow more than to radiative fog, because of its lack of stationarity.
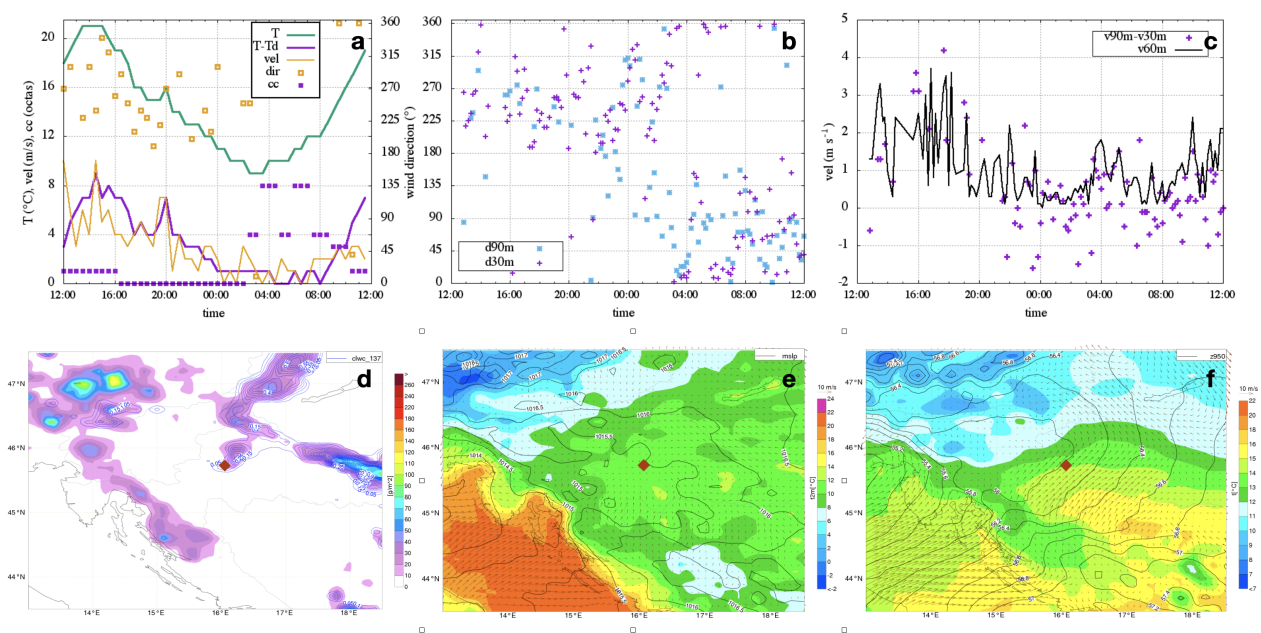

Figure 2. Summer intermittent fog on the Medvednica foothills, 17–18 September 2017. Top row: (**a**) half-hourly 24 h series of wind speed and direction at 10 m, T and dew point at 2 m, and cloud cover from ZGB METAR reports; (**b**) 15 min time series of wind direction at 10 m from METAR and 30 and 90 m from sodar; and (**c**) sodar wind speed at 60 m and speed difference between 90 and 30 m. Bottom row: (**d**) a zoom of ECMWF model centred in Zagreb (indicated by a rhombus) at 05 UTC showing fields of integrated liquid water contents 1 km above the surface; (**e**) 10 m wind, T2m and mean sea level pressure; and (**f**) geopotential height, wind, and T at 950 hPa.

The outputs of the ECMWF model for this day fit the observed evolution very well. The time series for Zagreb Airport are coherent with the description above, showing a shift for WSW to NE near 00 UTC with lower wind speeds (not shown). This change allows the development of fog in the model at this location between 3 and 7 UTC. Inspection of horizontal cross-sections in the area indicate that there is a well-defined wind from SW at 950 hPa at 05 UTC, while the wind from NE is weak at 10 m, and fog is formed at the foothills of Medvednica over the airport area (Figure 2d–f).

Therefore, both the available experimental information and the output of the ECMWF model at a relatively coarse horizontal resolution (9 km) indicate that when the general wind weakens and a downslope flow develops, this feature may be well correlated with the development of fog in summer over the airport area at the foothills, independently of how precisely the actual slope is seen by the ECMWF topography.

3.2. Generation of Fog in Winter by Gravity Flows

During the winter night 27–28 January 2018, Zagreb was under the centre of a high-pressure area, with weak regional winds veering from NE to SW along the night. METAR reports (Figure 3a) indicate Sc over Zagreb Airport from late afternoon (17 UTC) at a height of about 300 m agl until 23 UTC. Afterwards, higher clouds are reported and there is formation of mist later in the night. The wind at 10 m agl weakens during the evening blowing from ENE until 22 UTC, decreasing afterwards with NE direction (where the mountain range is) becoming almost calm in the second half of the night. The sodar data (Figure 3b,c) show that after 22 UTC, the wind profile has the form of a weak LLJ (speed at 30 m larger than at 90 m agl) coming from NE until 04 UTC and very variable afterwards. Therefore, when NE mesoscale wind vanishes, the development of a weak katabatic flow takes place, while at Zagreb Airport mist is reported with visibility reduced to less than 3 km.
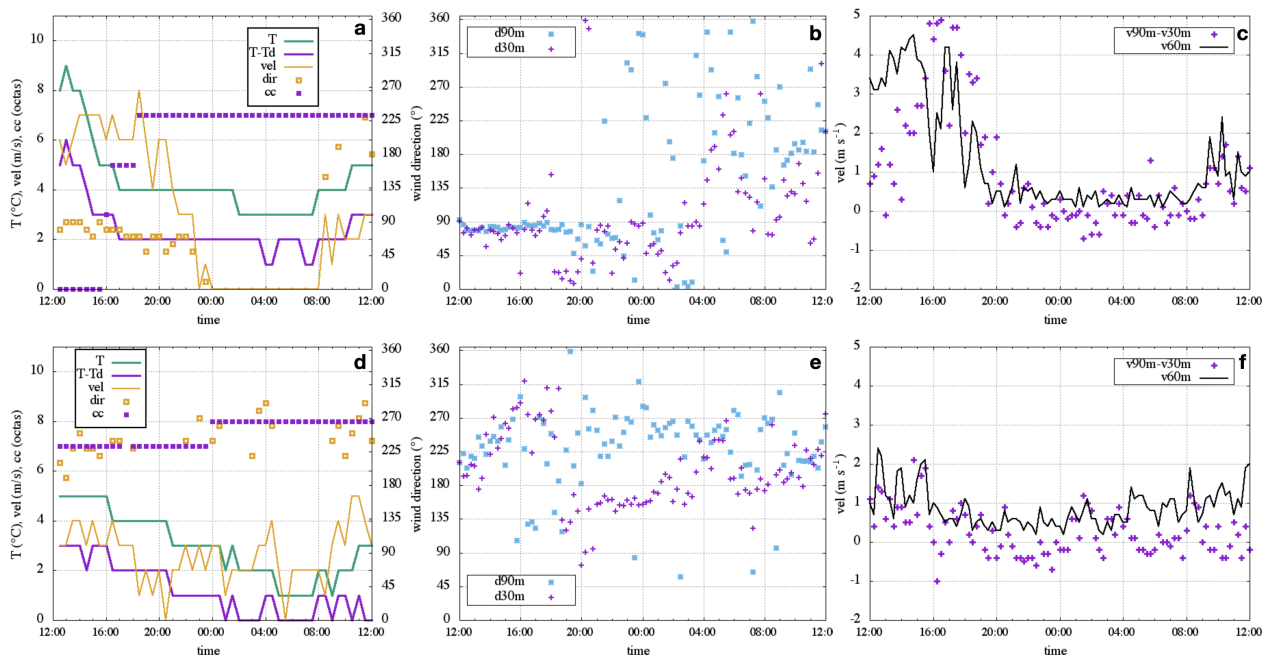

Figure 3. Sodar and METAR data at Zagreb Airport. For 27 to 28 January 2018: (**a**) half-hourly 24 h series of wind speed and direction at 10 m, T and dew point at 2 m, and cloud cover from Zagreb Airport METAR reports; (**b**) 15 min time series of wind direction at 10 m from METAR and 30 m and 90 m from sodar; (**c**) sodar wind speed at 60 m and speed difference between 90 and 30 m. In the lower row, the same figures (**d**–**f**) are shown for 28 to 29 January 2018.

The ECMWF model for this night does not lift the Sc clouds at midnight and the downslope flows are not generated. Instead, the WRF-ARW simulation captures the observed evolution with good approximation, with NE wind and cloud cover until 22 UTC, clearing the sky for a couple of hours afterwards until cloud cover is found again from 02 UTC on. The modelled evolution of wind, liquid water, and potential temperature for the clear skies in the interval 00 to 02 UTC is shown in Figure 4. During this period, a katabatic flow develops in the simulation and progresses over the plain at the foothills, creating a fog layer as it advances.

Figure 4a,d describe the situation at the beginning of the episode (00 UTC). Some banks of fog are formed in the area after the skies clear, most likely radiative fog, while the

downslope flow is in its initial stages, very shallow over the slopes and not having reached the foothills. One hour later (Figure 4b,e), the katabatic flow has advanced around 5 km over the foothills and we see a perfect overlap of the gravity flow and the fields of liquid water, which coincides with the top of the thermal inversion (not shown). The horizontal extension of the fog increases, most of it with winds blowing from the direction of the mountain range. At the end of the episode (Figure 4c,f), the fog continues extending as far as 20 km from the mountain, while its depth increases with the depth of the downslope flow.

The simulated events are compatible with the ones observed during that night between 00 and 02 UTC. This modelled katabatic event is singular because it is a cold start, responding to a sudden clearing of the skies. Between 01 and 02 UTC, the rate of horizontal progress over the plain is more than 10 km in one hour. If this progress rate was sustained, a katabatic developing in the evening could progress over the plain about 100 km away, and this distance could be around 150 km in a 15 h winter night in mid-latitudes. Therefore, this structure would become important at the mesobeta scale, and particularly for the Pannonian Basin, and the progression speed is in agreement with the one documented for the downslope flow from the Pyrenees over the Garonne basin [12].
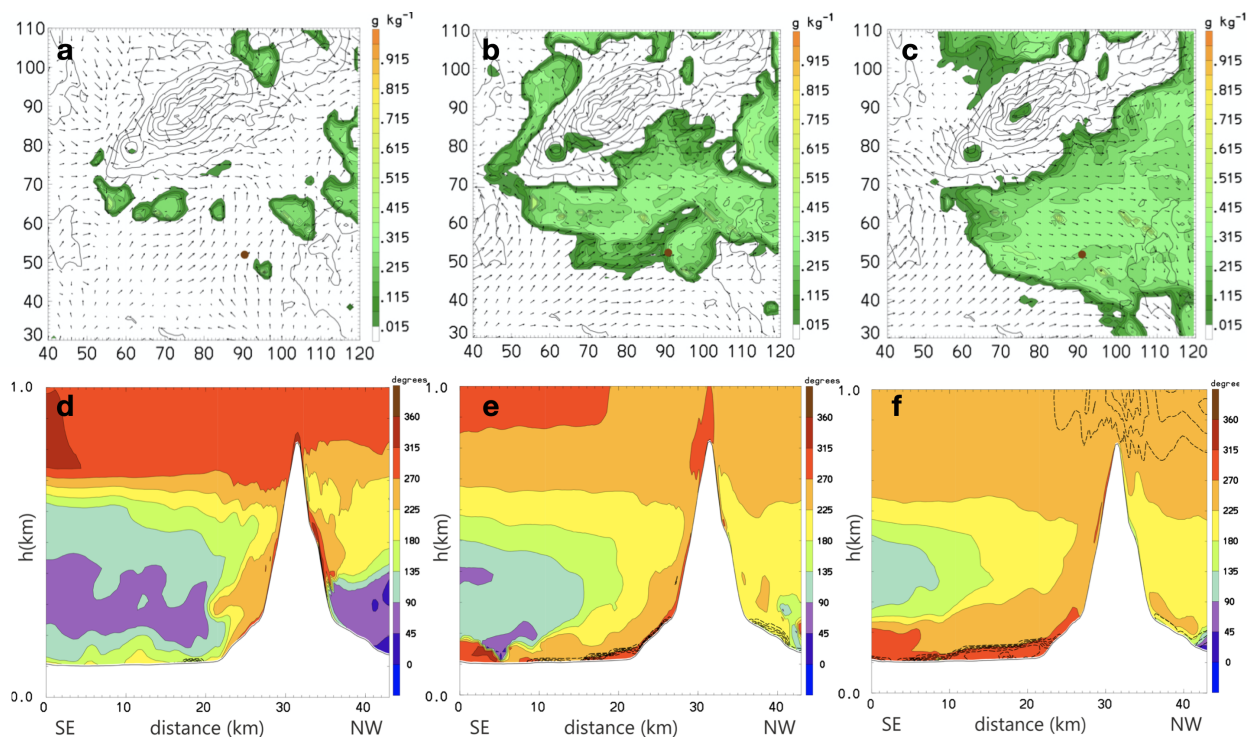

Figure 4. Katabatic event developing during the clear-skies interval of night 27–28 January 2018. Top: horizontal vector and cloud water (colour) at the first model level ((**a**) 00 UTC, (**b**) 01 UTC, (**c**) 02 UTC). Bottom: wind direction (colours) and cloud water (dashed lines) along the same line ((**d**) 00 UTC, (**e**) 01 UTC, (**f**) 02 UTC).

3.3. Interaction of Deep Fog Layers and Gravity Flows in Winter.

During the night on 28–29 January 2018, there is no well-defined synoptic gradient over the Zagreb region and, according to the METAR reports and the sodar data (Figure 3d–f), the wind at Zagreb Airport is from the southern sector, probably of mesoscale origin, as the sodar indicates a very weak low-level jet blowing from SE under a SW flow above. There is no hint of arrival of gravity flows from Medvednica at any level. The Sc layer covers the sky with its base at 300 m agl, and in the evening (from 15 UTC), the cloud base approaches gradually the ground until it becomes fog (at 23 UTC), which will remain until 11 UTC the next day.

The ECMWF model provides clear skies in the area, failing to generate the Sc cloud layer and, again, we analyse the high-resolution mesoscale simulation made with the WRF-ARW model, that generates successfully a Sc layer at 19 UTC that will stay in place until 12 UTC the next day, and some samples of the evolution are shown in Figure 5a–d. A downslope flow develops at late afternoon over the Medvednica slopes. At 17 UTC, a shallow gravity flow is present over the lower slopes blowing under the general SW wind in clear skies according to the model. However, at 19 UTC, as the ABL temperature decreases, the whole layer becomes saturated and well-mixed by turbulence of mechanical origin, establishing a 300 m deep fog layer which behaves like a Sc but in contact with the ground, covering most of the lower areas. The observations describe the same situation but the cloud is not reaching the ground until 23 UTC.
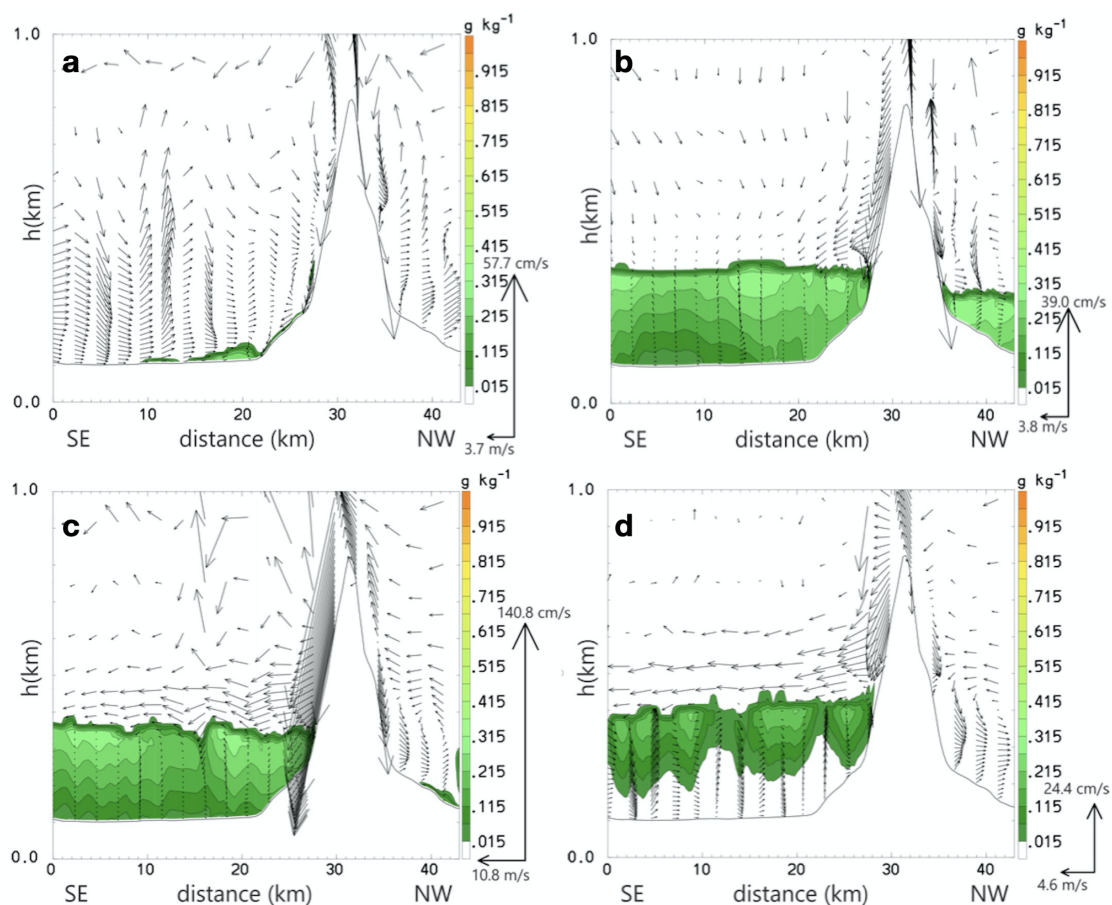

Figure 5. Deep fog layer on 28–29 January 2018: vertical cross-sections perpendicular to the Medvednica slope towards Zagreb Airport of wind vectors and cloud water at (**a**) 18 UTC, (**b**) 00 UTC, (**c**) 06 UTC, and (**d**) 11 UTC.

Once the Sc layer is in place, the situation will remain steady and the most interesting feature is that a katabatic flow develops at Medvednica above the cloud layer in the second part of the night, blowing over the Sc cloud deck and generating large wind shear at the upper inversion of the clouds and evidence of oscillations and, very likely, entrainment of dry air at some points. However, the height of the deck is not increasing with time, indicating the low quantitative importance of this effect due to the strong thermal inversion at the top of the Sc (about 7 K). This behaviour contrasts with the large entrainment rate in the Ebro fog case described in [22], where the elevated inversion of 4 K allowed significant entrainment and the fog increased in depth along time. The Sc fog layer will lift up from the bottom from 11 UTC, most likely due to the effect of solar radiation.

4. Basin-Scale Structure of the Nocturnal ABL and Fog Generation

In the previous section, we described how the gravity flows generated at the mountain slopes condition the nocturnal evolution of ABL in the foothills, particularly inducing fog events by mixing, and it was shown that the flows may progress over the plain at a significant speed, likely merging with valley flows. In this section, we discuss, first, the evolution of these flows as they blow away from the slopes and how they interact in the central part of the basin. Second, we describe the characteristics of the nocturnal ABL in the central part of the basin when cold air pools are formed, focusing on the surface thermal inversions and the generation of fog.

4.1. Topographically Generated Flows in Absence of Synoptic Pressure Gradient Over the Basin

Since the Pannonian Basin is surrounded by mountain ranges, the gravity flows generated in the slopes may merge with downvalley flows and meet at the central part of the basin if the appropriate meteorological conditions are given, which are essentially the lack of well-defined synoptic pressure gradients and the presence of clear skies.

Inspection of the ECMWF analyses over the basin for cases in these conditions suggests that the following classification in three main regions is possible, as described below for the night 2 to 3 September 2016 (Figure 6a). Furthermore, if there are well-defined pressure gradient between the basin and the surrounding regions to the N or the S, modifications to these patterns can occur.
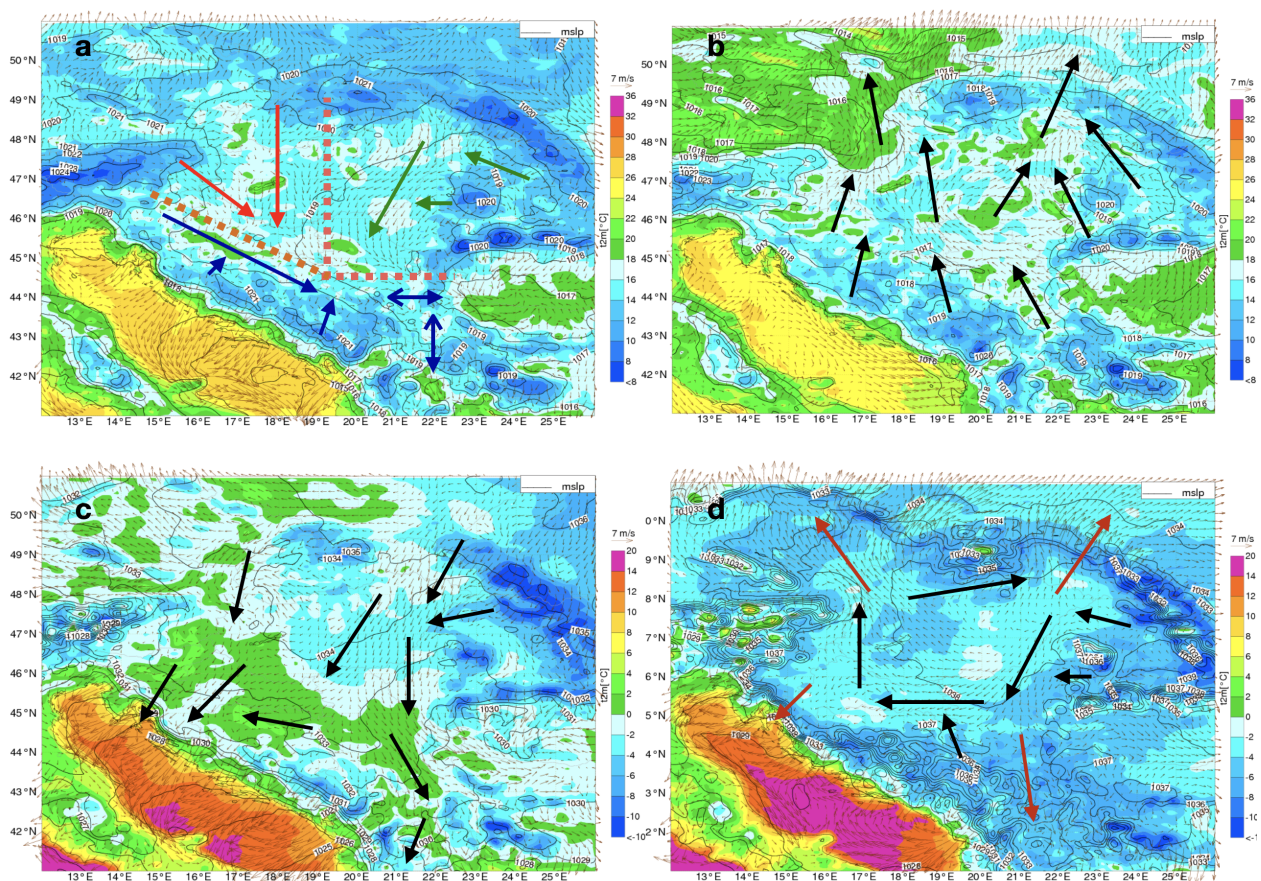

Figure 6. Different wind patterns when high pressure dominates over the Pannonian Basin (**a**) in the absence of well-defined pressure gradients (3 September 2016, 00 UTC), with red arrows in the Alpine-Drava region, green arrows in the Carpathian-Tisza region, blue arrows in the Dinarides-Sava region, and the dotted orange line roughly indicating the limits between these regions; (**b**) for lower pressure at the north (29 August 2016, 00 UTC); (**c**) for lower pressure at the south (16 December 2016, 00 UTC); and (**d**) for lower pressure regions at the north and south (22 December 2016, 00 UTC)—black arrows within-basin circulation, red arrows air that passes through outside the basin.

4.1.1. West: Eastern Alps, N–S Danube, and Drava Valleys

The influence of the Eastern Alps is mainly seen in the flows generated in the Drava valley and along the N–S part of the Danube. The Austrian part of the Drava flows through complicated topography and narrow valleys, and a clear downvalley flow is formed downwater of Maribor in Slovenia. This valley flow merges near Osijek with the N–S downvalley flow along the Danube that also collects the air from the slopes and valleys in the westernmost part of the Pannonian Basin. This N–S flow originates at the slopes of the northwestern Carpathians and reaches the Sava valley in absence of well-defined pressure gradients.

4.1.2. South: Dinarides, Sava, E–W Danube, and Great Morava Valleys

The Dinarides separate the Pannonian Basin from the Adriatic Sea; its southern side is where the Bora winds occur [37,38]. The mountain range has a width of about 50 km in its NW extreme, expanding to 150 km to the SW part. It is a wide elevated area with high mountain valleys and a very steep slope to the sea at the S and also a well-defined slope to the N down to the Sava Valley, which collects most of the downslope air at night. The air cumulated in the valley flows to E and rarely proceeds more to N, since the N–S downvalley flow along the Danube river or the NE–SW flow along the Tisza prevent it. Winds from this origin go usually as N as Szeged, as seen in the figure and as documented in [9]. The lower E–W Danube cannot flow freely through the narrow Iron Gates out of the basin, and this area is prone to air stagnation. However, when the downvalley flow from the Great Morava river reaches that area, the flow may become S or SE.

4.1.3. East: Carpathians, Transylvania, and the Tisza Valley

The Carpathians limit the Pannonian Basin to the N and surround the Transylvanian Plateau, which is partially open to the Alföld at the W, wherein the Apuseni mountains generate a narrow pass to the SW (Mures river) and a wider pass to the NW (Somes river). The plateau acts almost as a closed basin with a cold air pool (CAP) forming in clear and calm nights. The northwestern pass is of low altitude and allows the air to flow to the upper Tisza valley once the CAP becomes deep enough. The Tisza valley has a well-defined downvalley flow originating at the northeastern Carpathian foothills and reaching the lower Danube valley. It receives the flow from Transylvania in the N and the downslope and downvalley flows from the Apuseni mountains at the E.

4.1.4. How Do These Flows Meet?

These three major topographical wind systems usually meet in the central part of the basin, at the region near the city of Szeged, the circulation there depending of the relative strength of each of the incoming flows, which are conditioned by the meteorological conditions at their source areas. For instance, if there are clouds in the NW of the basin, the downvalley flow along the Danube will be weak or non-existent, and the southern flow may progress further N than explained, and the same reasoning applies for any other combination of effects on the three main areas.

4.1.5. Modifications Due to Large-Scale Pressure Gradients

Oftentimes, the presence of anticyclonic conditions over the Pannonian Basin goes together with significant differences in the pressure field over the regions surrounding it. It is very common to have lower pressure in the regions to the N, which results in the reversal of the downvalley flows in the N–S Danube valley, the Tisza valley, or both depending on the configuration of the pressure field. In this case, the downslope and downvalley flows generated at the S can proceed further north and even connect with the flows blowing outside the basin through the passes to the W and the E of the Northern Carpathians (Figure 6b).

When the lower pressure is over the Adriatic Sea (Figure 6c), the basin air flows S across the NW and SE extremes of the Dinarides, where there are topographical passes,

and the circulation along the lower Danube and the Sava river reverses as the flow cannot overpass the mountain and blows along the foothills to the NW until it can flow to the Adriatic. In addition, the downvalley flows generated along the N–S Danube and the Tisza valleys may connect with the flow blowing S.

When the pressure is lower both at the N and the S of the basin than over it, there is air blowing simultaneously to both areas, and a basin-wide anticyclonic-like circulation may be established (Figure 6d). This is the result of the outflow through the main passes at the four corners (Kvarner at SW, Montenegro at SE, Transcarpathia at NE, and the Bratislava region at NW), with the loss of ABL air having to be compensated by subsiding air coming from aloft.

Finally, if the high-pressure system implies the presence of pressure gradients over some part of the basin, the flow in the ABL will adjust to this gradient and the parts of the basin under no significant pressure gradient will function as described above.

4.2. Cold Air Pools

In clear skies and with weak synoptic winds, surface radiative cooling of the surface from late afternoon results in the progressive development of a surface-based thermal inversion. If air is topographically confined, this area is called a cold air pool (CAP). When the thermal inversion is destroyed the following morning, the phenomenon may repeat again the following evening if the same conditions are met [39]. This configuration often allows the generation of radiative or turbulent mixing fog along the night, that is dissipated in the morning.

In the case of summer nights, which are short, the seasonal dryness of the terrain favours strong temperature drops in the late afternoon and early evening with well-formed terrain flows and the creation of CAPs. However, in winter days when the solar irradiation is small and of short duration, temperature drops may be shorter than in summer, especially because water phase changes are usually more intense, releasing latent heat. Furthermore winter fog may not fully dissipate in the daytime, generating a persistent multi-day cold pool event with the presence of fog [22].

The exploration of ECMWF outputs for CAP events in the Pannonian Basin for the present study indicates that at the basin scale, CAPs form frequently, although radiation fog occurs also over some low-level areas. Instead, cloud-covered CAP events for the whole basin are normally related to turbulent mixing linked to mesoscale flows as the one described before for 29 January near Zagreb, generating a deep fog layer of a few hundred metres of depth, a situation that will be described below.

4.2.1. Clear-Skies Cold Air Pool

The case of the night 2–3 September 2016 is again taken here to inspect the characteristics of the CAP. The observed profiles at Szeged (Figure 7a–d) indicate an inversion in θ of about 10 °C up to 300 m agl, with winds at its upper part of 4–5 m/s from NE, the model more clearly marking a LLJ with the maximum speed at the top of the inversion. The basin-wide fields at 05 UTC of mean sea level pressure, temperature at 2 m, and wind at 10 m (Figure 7e) indicate the lack of pressure gradient, the dominancy of weak local winds, and distinct thermal areas in the Alföld and Transylvania. Inspection of the vertical cross-sections along the Tisza river down to the Dinarides (not shown), indicate that the vertical structure of wind and temperature is similar all along the line.

In winter, nights are longer, and the establishment of high-pressure systems usually results in the basin being covered by low clouds due to the high air moisture and the low temperatures. Nevertheless, it is possible to have clear-sky CAPs in winter if the air mass is relatively dry. Furthermore, the temperature drops along the night are usually smaller than in summer because the surface is more moist. During the night of 3 to 4 December 2016, the profiles in Figure 8a–d show a 4 °C inversion 200 m deep, containing a LLJ with maximum speed of 3–4 m/s from the NW. Above we see a residual well-mixed layer with

no wind. The vertical cross-section along the Tisza river valley (Figure 8e) indicates that the shallow inversion extends over the whole region.
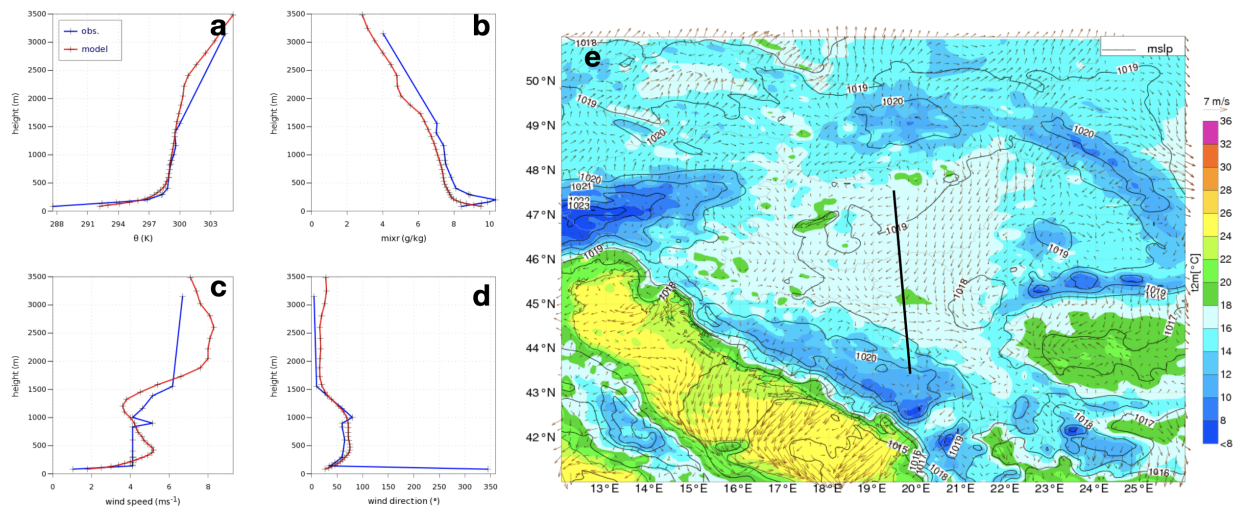

Figure 7. Summer clear skies cold air pool (2–3 September 2016): (**a**) radiosounding (blue) and ECMWF profile (red) at Szeged Airport at 00 UTC (blue) for potential temperature, (**b**) water vapour mixing ratio, (**c**) wind speed, and (**d**) wind direction; (**e**) temperature at 2 m and wind at 10 m in ECMWF output at 05 UTC, near sunrise. The black line indicates the location of the vertical cross-sections in Figures 8 and 9.
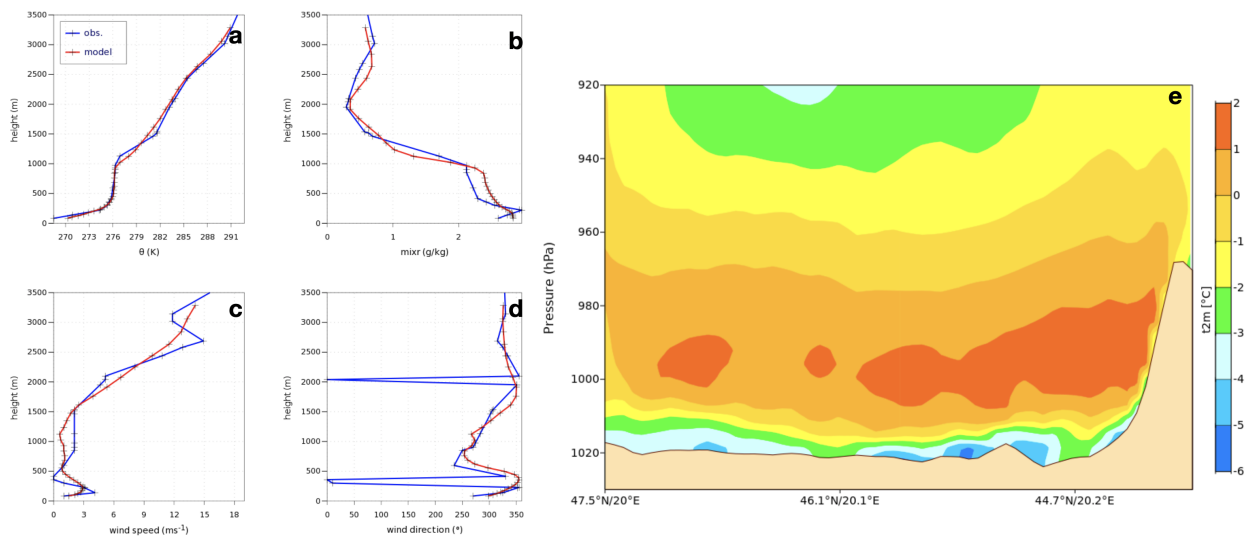

Figure 8. Winter clear skies cold air pool (3–4-December 2016): (**a**) radiosounding (blue) and ECMWF profile (red) at Szeged Airport at 00 UTC (blue) for potential temperature, (**b**) water vapour mixing ratio, (**c**) wind speed, and (**d**) wind direction; (**e**) potential temperature in the lower atmosphere near sunrise (06 UTC) along the Tisza river valley reaching the Dinarides.

4.2.2. Stratocumulus and Fog Covered Cold Air Pool

In situations when the high-pressure system implies low temperatures and high relative humidities, condensation in the ABL is easily reached, usually in form of a low Sc deck. An event lasting four days, 22 to 24 December 2016 is commented on. Figure 9a–f show that at the beginning of the event (22D), the fog extends as high as the LLJ, indicating that it is this structure that contributes to this formation. When the fog is mature (23D) it has become deeper, having a stronger thermal inversion at its top, and with contradictory information between the model and the radiosounding concerning the LLJ, the former having the maximum speed at the top of the cloud. These features are very similar to the ones found in the foothills of Medvednica by Zagreb, where the first night the LLJ was

generating the fog, and the second night the gravity flows blew above the cloud, causing an increase of its depth by entrainment. Therefore, we find similar mechanisms in the centre of the plain, far from the mountain ranges.

Figure 9g displays the horizontal extent that the event may reach, covering most of the basin, well constrained by the topography. The vertical cross-sections (Figure 9h,i) indicate that the Sc has its base very close to the surface and its vertical thermal structure is well mixed. At night, the cloud may touch the surface, generating a fog event, normally lifted at noon the day after.
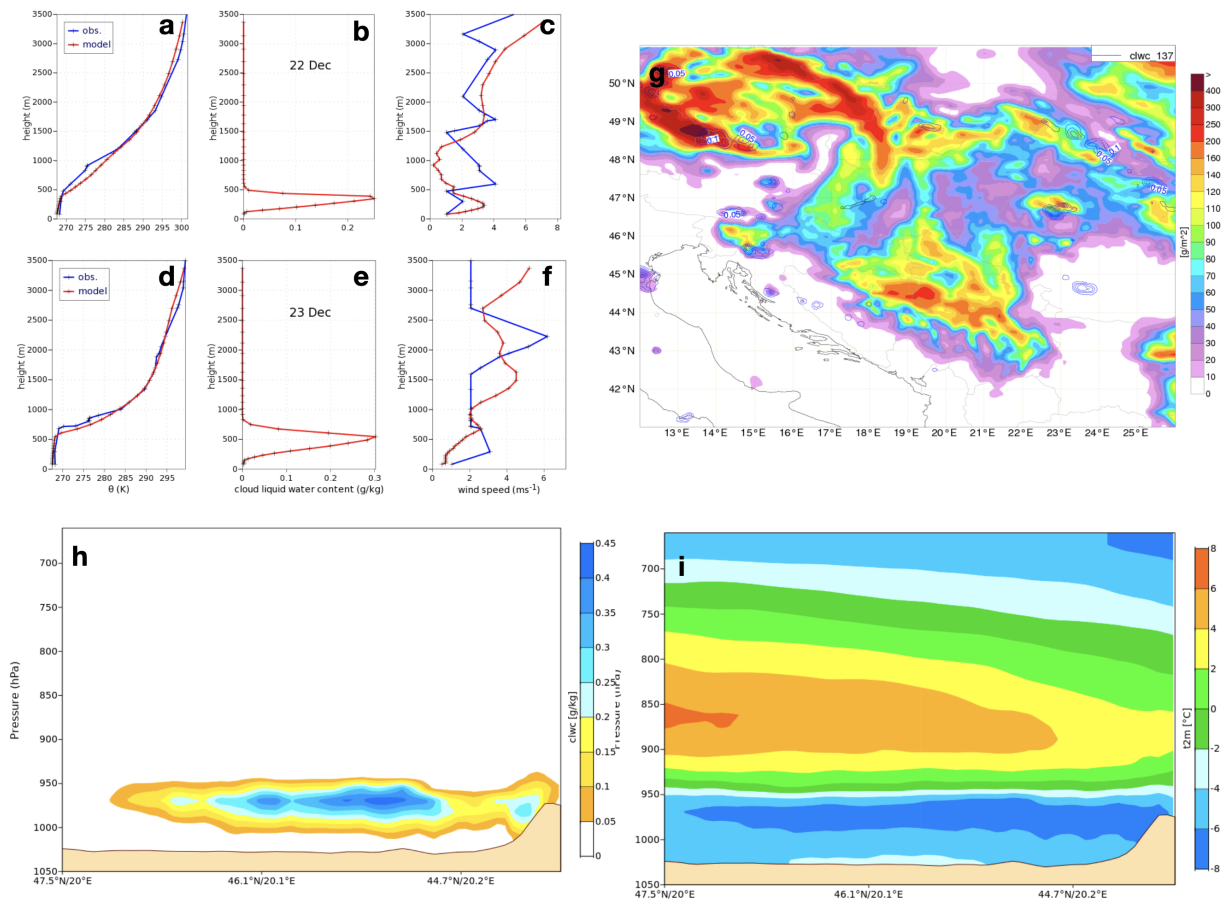

Figure 9. Winter stratocumulus and fog-covered cold air pool (22–24 December 2016): (**a**) radiosounding (blue) and ECMWF profile (red) at Szeged Airport at 00 UTC (blue) for potential temperature, (**b**) water vapour mixing ratio, (**c**) wind speed at 00 UTC of 22 December; (**d**–**f**) similarly for 00 UTC of 23 December; (**g**) maximal extension of the Sc deck at the end of the fog event (24 December 2016, 06 UTC) showing the integrated cloud water for the lower 600 m of the atmosphere; (**h**) vertical cross-sections of cloud water along the Tisza valley reaching the Dinarides of cloud water on 23 December at 00 UTC; (**i**) similarly for temperature.

5. Discussion

The three cases in the Zagreb area analysed here supplement the Telisman Prtenjak et al. study [8], with new backup experimental information provided by the sodar in the airport. The summer case shows that fog generation by the arrival of a downslope flow is also possible in the warm season, in this case with intermittent fog events. The first winter night illustrates a sudden development in the middle of the night of the downslope flow and allows estimating a propagation speed of the gravity flow over the plain, nearing 10 km h^{-1}. The second winter night shows that when the nocturnal ABL experiences condensation by cooling across its whole depth, a Sc cloud deck of a few hundreds of meters deep is formed that can become fog at night, and the downslope flows blow over them, causing entrainment.

Therefore, we identify, so far, three causes of generation of fog in the foothills area:

(i) radiative fog when the downslope flows do not reach the area and the skies are clear;

(ii) fog by turbulent mixing as the downslope flow reaches the area, that may remain in cold conditions and be dissipated in warm conditions;

(iii) establishment of a Sc cloud deck in the ABL that can touch ground along the night and lift in the central hours of the day

The characteristics of the downslope flow over the steep slope of Medvednica can be inspected using the values provided by the numerical model. The depth of the flow can be estimated as $D_{max} = \frac{-H}{v \sin(\alpha) \frac{d\theta}{dz}}$, where v is the maximum speed of the jet, H the sensible heat flux at the surface, α is the slope angle, and D_{max} is the maximum depth of the flow [40]. Taking values from the model at 02 UTC of January 28 (H = -22 W m^{-2}, v = 2 m s^{-1}, angle = 7°, $\frac{d\theta}{dz}$ = 0.01 K/m), the estimated depth of the downslope flow is of about 7 m.

Furthermore, the Froude number, computed as $Fr = \frac{v}{\sqrt{g'D}}$ [41], where $g' = \frac{\Delta\theta}{\theta_{ref}} g$ is the reduced gravity, using v = 2 m s^{-1}, $\Delta\theta$ = 0.05 K, g = 10 m s^{-2}, θ_{ref} = 300 m, and D = 7 m, provides a value well above 1, indicating that the flow will experience a hydraulic jump and lose continuity as it progresses downwards. Finally, the computation of the Bulk Richardson number $Ri_B = \frac{g\Delta\theta\Delta z}{\theta_{ref}(\Delta U^2 + \Delta V^2)}$, using the values above and considering $\Delta U^2 + \Delta V^2 = 1$ m^2 s^{-2}, gives $Ri_B = 0.01$, well below critical, indicating that the flow is in a turbulent regime. Customarily, the critical values for Fr and Ri_B are taken as 1 [42].

Unfortunately, the presence of fog in the lower part of the Medvenica mountain and on the plain do not allow computing D_{max} with the above expression, conceived for clear-sky conditions when the surface flux is well connected to the ABL dynamics, which is not the case in the presence of fog, driven mostly from processes at its top. For these two points, we estimate the depth of the flow from the model outputs. The vertical cross-sections show that there is a continuous downslope flow in the lower slopes (angle about 2°) of a maximum speed of the LLJ of 2 m/s at approximately of 30 m, providing a Froude number of 2, closer to the critical value (1) and $Ri_B = 0.3$. These parameters indicate that the downslope flow at this part is weakly turbulent, getting deeper and likely to experience a hydraulic jump. Over the plain, the model indicates a LLJ with a maximum speed of 2.2 m/s at a height of 50 m agl, a Fr number below critical, indicating continuity of the flow, and a Ri_B slightly under 1, a weakly turbulent regime.

Therefore, it can be considered that on the slopes, the flow is shallow with increasing depth, probably experiencing ruptures in its continuity in its way downhill. As the gravity flow reaches the plain in the form of a LLJ, it continues to gain depth as it progresses at a rate of 10 km per hour. This propagation speed, if adequate conditions were met (no impeding obstacles or opposing pressure gradients) would allow the flow to reach distances well away from the mountain ranges into the basin, likely merging with valley flows.

The inspection of the ECMWF fields indicates that downslope and downvalley flows exist at night in the absence of synoptic pressure gradients, the latter converging in the centre of the basin. It is likely that these structures are independently set in motion locally and connect themselves. The inspection of the vertical cross-sections does not show a horizontal thermal gradient in the basin allowing the development of mesoscale barocline flows since most of the low part of the basin is at very similar temperatures, while the model shows the presence of shallow LLJs, typically 100 to 300 m agl. This is similar to the downslope flows found in the plains to the North of the Pyrenees [12] and seems to give credit to the possibility of downslope flows from the mountain slopes and valleys travelling long distances over the low flat area.

The effect of the Coriolis force is not obvious as would be expected for flows blowing for distances up to 100 km for several hours. On the one hand, near the slopes the topographic forcing is the main effect and, especially in complex terrain, it can overcome the contribution of the Coriolis forcing as was shown for the sea breeze in Istria [43]. On the other hand, in the central part of basin, in the absence of well-defined pressure gradients one would expect that the wind experienced inertial oscillation. However, as shown for

the Duero basin [11], the convergence of topographically generated flows conducted along the valleys usually prevents this phenomenon to take place, as may be happening here. Although the ECMWF model at Szeged tends to make the wind turn clockwise in some cases, the observed data do not sustain such effect.

The presence of low pressure areas outside the Pannonian Basin implies that cold air may flow from it to these areas, similarly as to when a water container empties laterally as it becomes full. By continuity, the cold air within the basin is organised accordingly, implying that some low-level circulations may change, most of the flows blowing northward when there are lower pressures there and southward in when the low pressures are on the Adriatic Sea. In the case of lower pressures N and S the low-level flows seem to organise in an anticyclonic-like basin-wide circulation, the cold air flowing out throughout the four lowest corners of the basin.

Anticyclonic conditions are prone to the formation of CAPs. In summer and in dry winter cases, inversions are usually of the depth of the LLJ, and they can be as strong as 10 K in summer when the terrain is dry, while they are usually less strong in winter. For winter cases with high relative humidity, the LLJs provide the necessary turbulent mixing [44] to allow the nocturnal ABL to be well mixed, condensing in bulk when saturating conditions are met, generating large areas covered by Sc that may be basin-wide in the absence of synoptic-pressure gradients. This phenomenon prevents ground-based radiation fog to prevail under winter anticyclones. Instead, fog is formed at night when the Sc deck touches ground and lifts during the central hours of the day. This mechanism is similar to what was also found in the Ebro basin [22].

The outputs of the largest domain of WRF-ARW (not shown) indicate that the areas where the wind speed at 200 m agl is strongest coincide approximately with those which have the largest surface heat flux, showing that when LLJs are present there is turbulence for the depth of the nocturnal boundary layer, enhancing the heat exchange at the surface. The intensity of turbulence is related to the depth of the fog layer. Radiation fog a few tens of meters deep appears with weak winds and turbulence in the absence of well-defined LLJs. Instead, the deep fog layers observed to cover most of the Pannonian Basin in winter nights are the result of a nocturnal ABL well mixed by LLJs cooled below the saturation point, linked to the mesoscale basin circulations.

6. Conclusions

The large flat area of the Pannonian Basin is surrounded by mountain ranges and the Transylvanian elevated area. We have seen, using data from Zagreb Airport, that under high-pressure conditions and clear skies, downslope flows are generated at the mountain slopes and usually progress over the foothills. Their passage modifies the state of the nocturnal boundary layer as the air mass arriving has different thermodynamic characteristics, generates turbulent mixing and enhances the exchange fluxes between the surface and the atmosphere. The gravity flows can also induce a mixing fog event, sometimes overruling the pre-existing shallow radiation fog. If a dense fog layer is already on place, the katabatic flows may blow over the cloud deck causing turbulent mixing at its top.

These gravity flows progress over the low lands at a rate of a few kilometres per hour, contributing to valley flows. The ECMWF model outputs indicate that three main regions are at the origin of the flows converging at the central flat area are the eastern area limited by the Alps, the southern area limited by the Dinarides, and the northern and northwestern area limited by the Carpathians and including the Transylvanian elevated area. Depending on the meteorological conditions, the extent of each one of these systems may vary, and cloudiness or significant wind on one of the areas may deactivate the gravity flows there, leaving space for the others to progress further. The pressure pattern over the regions adjacent to the Pannonian Basin may modify these structures as the low-level air will tend to blow to lower pressure areas even if the local gradient is negligible.

The structure of the surface-based thermal inversion in the central area is linked to the presence of the mesoscale flows, since the top of the inversion in clear skies is usually at the top of mesoscale low-level jets. Fog formation in the centre of the basin can take place by radiative cooling, but it is normally restricted to some specific areas. The episodes when most of the basin is covered by low clouds or fog is usually in the wintertime, when the mesoscale flows experience condensation in their whole depth as temperature drops in the evening, with these episodes usually lasting several days, as fog is not dissipated in the daytime.

The conducted analysis has allowed discriminating that, in high-pressure conditions, shallow radiation fog only appears when no significant wind blows, a relatively rare situation at the basin scale but common locally. Furthermore, turbulent mixing related to downslope flows and mesoscale LLJs is able to generate fog layers as the air cools radiatively for the whole depth of the flow, tens of metres for downslope flows and a few hundreds of meters for LLJs. In the latter case, mesoscale circulations can explain basin-wide fog events in winter. Downslope flows and basin-scale LLJ circulations exist in both cold and warm seasons, but only in winter do they seem to lead very often to fog, while in summer the presence of fog is short lived or sporadic.

As most of these conclusions are based on numerical model outputs, backed by their consistency with the available observations, it would be advisable to proceed in a more systematic manner to study these phenomena. We would, on the one hand, recommend performing statistical analyses over the available databases to seek for further evidence of the mechanisms indicated here while, on the other hand, process-focused experimental campaigns would bring specific information for such investigations.

Author Contributions: J.C. designed the research concept, analysed the sodar and METAR data and wrote the bulk of the manuscript. M.T.P. designed, run and analysed the outputs of the high-resolution WRF-ARF simulations, also producing the related figures while contributing to the scientific discussion and editing the manuscript. B.M. obtained the ECMWF data and generated the necessary numerical and graphical outputs for the analysis. All authors have read and agreed to the published version of the manuscript.

Institutional Review Board Statement: Not applicable.

Informed Consent Statement: Not applicable.

Data Availability Statement: The Croatian Meteorological and Hydrological Service generated the METAR and SYNOP data at Zagreb Airport and owns the Sodar data. Data at Szeged airport was generated by the Hungarian Meteorological Service.

Conflicts of Interest: The authors declare no conflict of interest.

References

1. Ceglar, A.; Croitoru, A.E.; Cuxart, J.; Djurdjevic, V.; Güttler, I.; Ivancan-Picek, B.; Jug, D.; Lakatos, M.; Weidinger, T. PannEx: The Pannonian Basin Experiment. *Clim. Serv.* **2018**, *11*, 78–85. [CrossRef]
2. Jug, D.; Djurdjevic, B.; Birkas, M.; Brozovic, B.; Lipiec, J.; Vukadinovic, V.; Jug, I. Effect of conservation tillage on crop productivity and nitrogen use efficiency. *Soil Tillage Res.* **2019**, *194*, 104327. [CrossRef]
3. Croitoru, A.E.; Man, T.C.; Vatca, S.D.; Kobulniczky, B.; Stoian, V. Refining the Spatial Scale for Maize Crop Agro-Climatological Suitability Conditions in an Area with Complex Topography towards a Smart and Sustainable Agriculture. Case Study: Central Romania (Cluj County). *Sustainability* **2020**, *12*, 2783. [CrossRef]
4. Szabo, A.I.; Acs, F.; Breuer, H. Larger Carpathian Region Climate According to Koeppen, Feddema and the Worldwide Bioclimatic Classification System methods. *Int. J. Climatol.* **2021**, *41*, E2482–E2496. [CrossRef]

5. Omazic, B.; Telisman Prtenjak, M.; Prsa, I.; Vozila, A.B.; Vucetic, V.; Karoglan, M.; Prsa, Z.; Anic, M.; Simon, S.; Guettler, I. Climate change impacts on viticulture in Croatia: Viticultural zoning and future potential. *Int. J. Climatol.* **2020**, *40*, 5634–5655. [CrossRef]
6. Lakatos, M.; Weidinger, T.; Hoffmann, L.; Bihari, Z.; Horvath, A. Computation of daily Penman-Monteith reference evapotranspiration in the Carpathian Region and comparison with Thornthwaite estimates. *Adv. Sci. Res.* **2020**, *16*, 251–259. [CrossRef]
7. Kalmar, T.; Pieczka, I.; Pongracz, R. A sensitivity analysis of the different setups of the RegCM4. 5 model for the Carpathian Region. *Int. J. Climatol.* **2021**, E1180–E1201.
8. Prtenjak, M.T.; Klaic, M.; Jericevic, A.; Cuxart, J. The interaction of the downslope winds and fog formation over the Zagreb area. *Atmos. Res.* **2018**, *214*, 213–227. [CrossRef]
9. Cuxart, J.; Tatrai, D.; Weidinger, T.; Kircsi, A.; Jozsa, J.; Kiss, M. Infrasound as a detector of local and remote turbulence. *Bound. Layer Meteorol.* **2016**, *159*, 185–192. [CrossRef]
10. Zardi, D.; Whiteman, C.D. Diurnal mountain wind systems. In *Mountain Weather Research and Forecasting*; Chow, F., De Wekker, S., Snyder, B., Eds.; Springer: Dordrecht, The Netherlands, 2013; pp. 35–119.
11. Cuxart, J. Nocturnal basin low-level jets: An integrated study. *Acta Geophysica* **2008**, *56*, 100–113. [CrossRef]
12. Jimenez, M.A.; Cuxart, J. A study of the nocturnal flows generated in the north side of the Pyrenees. *Atmos. Res.* **2014**, *145*, 244–254. [CrossRef]
13. Martinez, D.; Jimenez, M.A.; Cuxart, J.; Mahrt, L.Heterogeneous nocturnal cooling in a large basin under very stable conditions. *Bound. Layer Meteorol.* **2010**, *137*, 97–113. [CrossRef]
14. Cuxart, J.; Cunillera, J.; Jimenez, M.A.; Martinez, D.; Molinos, F.; Palau, J.L. Study of mesobeta basin flows by remote sensing. *Bound. Layer Meteorol.* **2012**, *143*, 143–158. [CrossRef]
15. Kysely, J.; Domonkos, P. Recent increase in persistence of atmospheric circulation over Europe: Comparison with long-term variations since 1881. *Int. J. Climatol.* **2006**, *26*, 46–483. [CrossRef]
16. Sfîca, L.; Croitoru, A.E.; Iordache, I.; Ciupertea, A.F. Synoptic conditions generating heat waves and warm spells in Romania. *Atmosphere* **2017**, *8*, 50. [CrossRef]
17. Baranka, G.; Bartók, B.; Bozó, L.; Croitoru, A.; Ferenczi, Z.; Firanj, Sremac, A.; Grisogono, B.; Jericevic, A.; Labancz, K.; Lalic, B.; et al. *Understanding Air Quality under Different Weather and Climate Conditions in the Pannonian Basin*; Eötvös Loránd University-Department of Meteorology: Budapest, Hungary, 2017; p. 67.
18. Jericevic, A.; Gasparac, G.; Mikulec, M.M.; Kumar, P.; Prtenjak, M.T. Identification of diverse air pollution sources in a complex urban area of Croatia. *J. Environ. Manag.* **2019**, *243*, 67–77. [CrossRef]
19. Lalic, B.; Eitzinger, J.; Mihailovic, D.T.; Thaler, S.; Jancic, M. Climate change impacts on winter wheat yield change-which climatic parameters are crucial in Pannonian lowland? *J. Agric. Sci.* **2013**, *151*, 757. [CrossRef]
20. Price, J.D. On the formation and development of radiation fog: An observational study. *Bound. Layer Meteorol.* **2019**, *172*, 167–197. [CrossRef]
21. Gultepe, I.; Tardif, R.; Michaelides, S.C.; Cermak, J.; Bott, A.; Bendix, J.; Müller, M.D.; Pagowski, M.; Hansen, B.; Ellrod, G.; et al. Fog research: A review of past achievements and future perspectives. *Pure Appl. Geophys.* **2007**, *164*, 1121–1159. [CrossRef]
22. Cuxart, J.; Jimenez, M.A. Deep radiation fog in a wide closed valley: Study by numerical modeling and remote sensing. *Pure Appl. Geophys.* **2012**, *169*, 911–926. [CrossRef]
23. Zhou, Y.; Bai, Y.; Yue, Y.; Lu, J.; Chen, S.; Xiao, H. Characteristics of the factors influencing transportation and accumulation processes during a persistent pollution event in the middle reaches of the Yangtze River, China. *Atmos. Pollut. Res.* **2019**, *10*, 1420–1434. [CrossRef]
24. Decesari, S.; Sowlat, M.H.; Hasheminassab, S.; Sandrini, S.; Gilardoni, S.; Facchini, M.C.; Fuzzi, S.; Sioutas, C. Enhanced toxicity of aerosol in fog conditions in the Po Valley, Italy. *Atmos. Chem. Phys.* **2017**, *17*, 7721–7731. [CrossRef]
25. Zoldos, M.; Jurkovic, J. Fog event climatology for Zagreb Airport. *Hrvatski Meteoroloski Casopis* **2016**, *51*, 13–26.
26. Skamarock, W.C.; Klemp, J.B.; Dudhia, J.; Gill, D.O.; Barker, D.M.; Wang, W.; Powers, J.G. A description of the Advanced Research WRF version 3. In *NCAR Technical Note-475+ STR*; National Center for Atmospheric Research (NCAR): Boulder, CO, USA, 2008.
27. Dudhia, J. Numerical study of convection observed during the winter monsoon experiment using a mesoscale two-dimensional model. *J. Atmos. Sci.* **1989**, *46*, 3077–3107. [CrossRef]
28. Mlawer, E.J.; Taubman, S.J.; Brown, P.D.; Iacono, M.J.; Clough, S.A. Radiative transfer for inhomogeneous atmospheres: RRTM, a validated correlated-k model for the longwave. *J. Geophys. Res. Atmos.* **1997**, *102*, 16663–16682. [CrossRef]
29. Janjic, Z.I. The step-mountain eta coordinate model: Further developments of the convection, viscous sublayer, and turbulence closure schemes. *Mon. Weather Rev.* **1994**, *122*, 927–945. [CrossRef]
30. Morrison, H.; Curry, J.A.; Khvorostyanov, V.I. A new double-moment microphysics parameterization for application in cloud and climate models, part I: Description. *J. Atmos. Sci.* **2005**, *62*, 1665–1677. [CrossRef]
31. Dudhia, J. A multi-layer soil temperature model for MM5. In Proceedings of the Sixth PSU/NCAR Mesoscale Model Users' Workshop, Boulder, CO, USA, 22–24 July 1996; pp. 22–24.
32. Nakanishi, M.; Niino, H. Development of an improved turbulence closure model for the atmospheric boundary layer. *J. Meteorol. Soc. Jpn.* **2009**, *87*, 895–912. [CrossRef]
33. Kusaka, H.; Kondo, H.; Kikegawa, Y.; Kimura, F. A simple single-layer urban canopy model for atmospheric models: Comparison with multi-layer and slab models. *Bound. Layer Meteorol.* **2001**, *101*, 329–358. [CrossRef]

34.	Román-Cascón, C.; Yagüe, C.; Sastre, M.; Maqueda, G.; Salamanca, F.; Viana, S. Observations and WRF simulations of fog events at the Spanish Northern Plateau. *Adv. Sci. Res.* **2012**, *8*, 11–18. [CrossRef]

35.	Román-Cascón, C.; Steeneveld, G.J.; Yagüe, C.; Sastre, M.; Arrillaga, J.A.; Maqueda, G. Forecasting radiation fog at climatologically contrasting sites: Evaluation of statistical methods and WRF. *Q. J. R. Meteorol. Soc.* **2016**, *142*, 1048–1063. [CrossRef]

36.	Steeneveld, G.J.; Ronda, R.J.; Holtslag, A.A.M. The challenge of forecasting the onset and development of radiation fog using mesoscale atmospheric models. *Bound. Layer Meteorol.* **2016**, *154*, 265–289. [CrossRef]

37.	Grisogono, B.; Belusic, D. A review of recent advances in understanding the mesoand microscale properties of the severe Bora wind. *Tellus A* **2009**, *61*, 1–16. [CrossRef]

38.	Belusic, A.; Prtenjak, M.T.; Guettler, I.; Ban, N.; Leutwyler, D.; Schar, C. Near-surface wind variability over the broader Adriatic region: Insights from an ensemble of regional climate models. *Clim. Dyn.* **2018**, *50*, 4455–4480. [CrossRef]

39.	Conangla, L.; Cuxart, J.; Jimenez, M.A.; Martínez-Villagrasa, D.; Miro, J.R.; Tabarelli, D.; Zardi, D. Cold-air pool evolution in a wide Pyrenean valley. *Int. J. Climatol.* **2018**, *38*, 2852–2865. [CrossRef]

40.	Cuxart, J.; Martinez-Villagrasa, D.; Stiperski, I. Validation of a simple diagnostic relationship for downslope flows. *Atm. Sci. Lett.* **2020**, *21*, e965. [CrossRef]

41.	Durran, D.R.; Klemp, J.B. Another look at downslope winds. Part II: Nonlinear amplification beneath wave-overturning layers. *J. Atmos. Sci.* **1987**, *44*, 3402–3412. [CrossRef]

42.	Stull, R.B. *An Introduction to Boundary Layer Meteorology*; Springer Science and Business Media: Dordrecht, The Netherlands, 1988; p. 666.

43.	Prtenjak, M.T.; Pasaric, Z.; Orlic, M.; Grisogono, B. Rotation of sea/land breezes along the northeastern Adriatic coast. *Ann. Geophys.* **2008**, *26*, 1711–1724. [CrossRef]

44.	Cuxart, J.; Jimenez, M.A. Mixing processes in a nocturnal low-level jet: An LES study. *J. Atmos. Sci.* **2007**, *64*, 1666–1679. [CrossRef]